G. L. Klimchitskaya*, S. I. Zanette, and A. O. Caride
Centro Brasileiro de Pesquisas Físicas, Rua Dr. Xavier Sigaud, 150
Urca 22290–180, Rio de Janeiro, RJ — Brazil

We find the lateral projection of the Casimir force for a configuration of a sphere above a corrugated plate. This force tends to change the sphere position in the direction of a nearest corrugation maximum. The probability distribution describing different positions of a sphere above a corrugated plate is suggested which is fitted well with experimental data demonstrating the nontrivial boundary dependence of the Casimir force.

12.20.Ds, 12.20.Fv, 61.16.Ch, 03.70.+k

Considerable recent attention has been focused on the Casimir effect [1,2]. On the theoretical side much work was done to investigate the corrections to the Casimir force due to the finite conductivity of the boundary metal [3–6], nonzero temperature [7–9], and surface roughness [10–12]. In the experimental field the new precision measurements of the Casimir force between metallic surfaces of a plane disk and a spherical lens (or a sphere) were performed [13–16]. The experimental results correlate well with the theoretical expressions taking into account all the corrections mentioned above. This provided a way to obtain new stronger constraints on the constants of Yukawa-type additional terms to Newtonian gravitational law predicted by the unified gauge theories, supersymmetry, supergravity, and string theory [17–21]. The Casimir effect has assumed a new meaning as a tool for investigation of fundamental interactions and their unification. Because of this, the detailed analyses of the fit of the theory to the data takes on great significance.

In Ref. [22] the Casimir force between an aluminum coated plate with sinusoidal corrugations and a large sphere was measured using an atomic force microscope. It was concluded that the measured force shows significant deviation from the perturbative theory which takes into account the periodic corrugation of the plate in the surface separation. In the absence of corrugations the same theory shows good agreement with the measured Casimir force. These together were considered in [22] to represent the nontrivial boundary dependence of the Casimir force and until recently has no theoretical explanation (in line with [22] dependence of this kind is to be expected due to diffractive effects associated with corrugated surface).

Here we present the perturbative calculation for both vertical and lateral Casimir force acting in the configuration of a sphere situated above a corrugated plate (note that the lateral force arises due to the absence of translational symmetry on a plate with corrugations). Our study revealed that the lateral force acts upon the sphere in such a way that it tends to change its position in the direction of a nearest maximum point of the vertical Casimir force (which coincides with the maximum point of corrugations). In consequence of this, the assumption made in [22] that the locations of the sphere above different points of a corrugated surface are equally probable can be violated. As indicated below, the diverse assumptions on the probability distribution describing location of the sphere above different points of the plate result in an essential change in force-distance relation. In such a manner the perturbation theory taking the lateral force into account may work for a case of corrugated plate. Notice that the fundamental importance of the lateral Casimir force acting between the corrugated boundaries was discussed in [23–25].

We start with the configuration of polystyrene sphere above a $7.5\times7.5\,\mathrm{mm}^2$ plate with periodic uniaxial sinusoidal corrugations. Both the sphere and the plate were coated with 250 nm of Al, and 8 nm layer of Au/Pd. For the outer Au/Pd layer transparencies greater than 90% were measured at characteristic frequences contributing into the Casimir force. The diameter of the sphere was $2R=(194.6\pm0.5)\,\mu$m. The surface of the corrugated plate is described by the function

$$z_s(x,y)=A\sin\frac{2\pi x}{L}, \tag{1}$$

where the amplitude of the corrugation is $A=(59.4\pm2.5)\,$nm and its period is $L=1.1\,\mu$m. The mean amplitude of the stochastic roughness on the corrugated plate was $A_p=4.7\,$nm, and on the sphere bottom — $A_s=5\,$nm.

As is seen from Eq. (1) the origin of the z-axis is taken such that the mean value of the corrugation is zero. We represent by a the separation between the zero corrugation level and the sphere bottom as they are not taking into

*On leave from North-West Polytechnical Institute,St.Petersburg, Russia. Electronic address: galinak@fisica.ufpb.br

account the surface roughness. The minimal value of a is determined, approximatelly, by $a_0 \approx A + A_p + A_s + 2h \approx 130\,\mathrm{nm}$, where $h \approx 30\,\mathrm{nm}$ is the height of the highest occasional rare Al crystals which prevent the intimate contact between the sphere bottom and the maximum point of the corrugation. The independent measurement of a_0 by use of electrostatic force results in $a_0 = (132 \pm 5)\,\mathrm{nm}$ [22]. For the case of the Casimir force measurements, i.e. with the addition of two transparent Au/Pd layers, this leads to $a_0 = (148 \pm 5)\,\mathrm{nm}$. We consider here the measurement data in the interval $164.5\,\mathrm{nm} \leq a \leq 400\,\mathrm{nm}$ (for larger a the Casimir force is less than the experimental uncertainty).

Let us take up first the vertical Casimir force acting between a corrugated plate and a sphere. A sinusoidal corrugation of Eq. (1) leads to the modification of the Casimir force between a flat plate and a sphere. The modified force can be calculated by the averaging over the period

$$F(a) = \int_0^L dx \rho(x)\, F_{ps}\left(d(a,x)\right). \tag{2}$$

Here $d(a,x)$ is the separation between the sphere bottom and the point x on the surface of corrugated plate

$$d(a,x) = a - A_p - A_s - A\sin\frac{2\pi x}{L}. \tag{3}$$

F_{ps} is the Casimir force acting between a flat plate and a sphere with account of corrections due to finite conductivity of the boundary metal [6]

$$F_{ps}(d) = F_{ps}^{(0)}(d)\sum_{i=0}^{4} c_i \left(\frac{\delta_0}{d}\right)^i, \tag{4}$$

where $F_{ps}^{(0)}(d) = -\pi^3 R\hbar c/(360a^3)$ is the same force for a perfect metal, and the numerical coefficients are

$$c_0 = 1, \quad c_1 = -4, \quad c_2 = \frac{72}{5}, \quad c_3 = -\frac{320}{7}\left(1 - \frac{\pi^2}{210}\right), \quad c_4 = -\frac{400}{3}\left(1 - \frac{163\pi^2}{7350}\right). \tag{5}$$

Note that the temperature corrections are neglegible at the separations under consideration. The quantity δ_0 from (4) is the penetration depth of the zero-point oscillations into the metal given by $\delta_0 = \lambda_p/(2\pi)$, λ_p is the plasma wavelength ($\lambda_p \approx 100\,\mathrm{nm}$ for Al). Note that Eq. (4) was obtained by means of Proximity Force Theorem [26] and perturbation expansion of the Lifshitz expression for the Casimir energy between two plane parallel plates.

The quantity $\rho(x)$ from Eq. (2) describes the probability distribution of the sphere positions above different points x belonging to one corrugation period. In [22] the uniform distribution was assumed ($\rho(x) = 1/L$) which is to say that the sphere is located above all points x belonging to the interval $0 < x < L$ with equal probability. The right-hand side of Eq. (2) was expanded in powers of a small parameter $A/(a - A_p - A_s)$. This expansion had shown significant deviations from the measured data while Eq. (4) is in excellent agreement with data for all $d \geq \lambda_p$ [6] in the limit of zero amplitude of corrugation.

Now we turn to the lateral projection of the Casimir force which was not considered in [22]. The lateral projection is nonzero only in the case of nonzero corrugation amplitude. In [22] neither the lateral force nor the force constant relative to the horizontal displacement of a cantilever were measured. Because of this it is not reasonable to develop the complete theory describing the shifts of a sphere under the influence of a lateral Casimir force and giving the possibility to find theoretically the probability distribution $\rho(x)$ from Eq. (2). In this connection we restrict ourselves to calculation of the lateral force in the simplest case of the ideal metal.

This can be achieved by applying the additive summation method of the retarded interatomic potentials over the volumes of a corrugated plate and a sphere with subsequent normalization of the interaction constant [5,11,12]. Alternatively the same result is obtainable by the Proximity Force Theorem [26] (for the case of the nonretarded van der Waals force these approaches were applied, e.g., in [27]). Let an atom of a sphere be situated at a point with the coordinates (x_A, y_A, z_A) in the coordinate system described above. Integrating the interatomic potential $V = -C/r_{12}^7$ over the volume of corrugated plate (r_{12} is a distance between this atom and the atoms of a plate) and calculating the lateral force projection according to $-\partial V/\partial x_A$ one obtains [11,12]

$$F_x^{(A)}(x_A, y_A, z_A) = \frac{4\pi^2 n_p C}{5z_A^5}\,\frac{A}{z_A}\,\frac{z_A}{L}\left[\cos\frac{2\pi x_A}{L} + \frac{5}{2}\,\frac{A}{z_A}\sin\frac{4\pi x_A}{L}\right], \tag{6}$$

where n_p is the atomic density of a corrugated plate. Eq. (6) is obtained by perturbation expansion of the integral (up to second order) in small parameter A/z_A.

We can represent $x_A = x_0 + x$, $y_A = y_0 + y$, $z_A = z_0 + z$ where (x_0, y_0, z_0) are the coordinates of the sphere bottom in the above coordinate system, and (x, y, z) are the coordinates of the sphere atom in relation to the sphere bottom. The lateral Casimir force acting upon a sphere is calculated by the integration of (6) over the sphere volume and subsequent division by the normalization factor $K = 24Cn_p n_s/(\pi\hbar c)$ obtained by comparison of additive and exact results for the configuration of two plane parallel plates [5]

$$F_x(x_0, y_0, z_0) = \frac{n_s}{K} \int\limits_{V_s} d^3r \, F_x^{(A)}(x_0 + x, y_0 + y, z_0 + z), \tag{7}$$

where n_s is the atomic density of sphere metal.

Let us substitute Eq. (6) into Eq. (7) neglecting the small contribution of the upper semisphere which is of order $z_0/R < 4 \times 10^{-3}$ comparing to unity. In a cylindrical coordinate system the lateral force acting upon a sphere rearranges to the form

$$F_x(x_0, y_0, z_0) = \frac{\pi^3\hbar c}{30}\frac{A}{L}\left[\cos\frac{2\pi x_0}{L}\int\limits_0^R \rho d\rho \int\limits_0^{R-\sqrt{R^2-\rho^2}} \frac{dz}{(z_0+z)^5}\int\limits_0^{2\pi} d\varphi \cos\left(\frac{2\pi\rho}{L}\cos\varphi\right)\right.$$
$$\left. + \frac{5}{2}A\sin\frac{4\pi x_0}{L}\int\limits_0^R \rho d\rho \int\limits_0^{R-\sqrt{R^2-\rho^2}} \frac{dz}{(z_0+z)^6}\int\limits_0^{2\pi} d\varphi \cos\left(\frac{4\pi\rho}{L}\cos\varphi\right)\right]. \tag{8}$$

Using the standard formulas from [28] the integrals with respect to φ and z are taken explicitly. Preserving only the lowest order terms in small parameter $x_0/R < 10^{-2}$ we arrive at

$$F_x(x_0, y_0, z_0) = -\frac{\pi^4\hbar c}{60 z_0^4}\frac{A}{L}\left[\cos\frac{2\pi x_0}{L}\int\limits_0^R \rho d\rho J_0\left(\frac{2\pi\rho}{L}\right) + 2\frac{A}{z_0}\sin\frac{4\pi x_0}{L}\int\limits_0^R \rho d\rho J_0\left(\frac{4\pi\rho}{L}\right)\right], \tag{9}$$

where $J_n(z)$ is Bessel function.

Integrating in ρ the final result is obtained

$$F_x(x_0, y_0, z_0) = 3F_{ps}^{(0)}(z_0)\frac{A}{z_0}\left[\cos\frac{2\pi x_0}{L}\, J_1\left(\frac{2\pi R}{L}\right) + \frac{A}{z_0}\sin\frac{4\pi x_0}{L}\, J_1\left(\frac{4\pi R}{L}\right)\right], \tag{10}$$

where the vertical Casimir force $F_{ps}^{(0)}$ for ideal metal was defined after Eq. (4).

As is seen from Eq. (10) the lateral Casimir force takes zero value at the extremum points of the corrugation described by Eq. (1). The lateral force achieves maximum at the points $x_0 = 0$, $L/2$ where the corrugation function is zero. If the sphere is situated to the left of a point $x_0 = L/4$ (maximum of corrugation) it experiences a positive lateral Casimir force. If it is situated to the right of $x_0 = L/4$ the lateral Casimir force is negative. In both cases the sphere tends to change its position in the direction of a corrugation maximum which is the position of stable equilibrium. The situation here is the same as for an atom near the wall covered by the large-scale roughness [11]. That is the reason why the different points of a corrugated plate are not equivalent and the assumption that the locations of the sphere above them are described by the uniform probability distribution may be unjustified.

On this basis, one may suppose that the probability distribution under consideration is given by

$$\rho(x) = \begin{cases} \frac{2}{L}, & kL \le x \le \left(k+\frac{1}{2}\right)L, \\ 0, & \left(k+\frac{1}{2}\right)L \le x \le (k+1)L, \end{cases} \tag{11}$$

where $k = 0, 1, 2, \ldots$ This would mean that in the course of the measurements the sphere is located with equal probability above different points of the convex part of corrugation but cannot be located above the concave one.

It is even more reasonable to suppose that the function ρ increases by the linear law when the sphere approaches the points of a stable equilibrium. In this case the functional dependence is given by

$$\rho(x) = \begin{cases} \frac{16}{L^2}x, & kL \le x \le \left(k+\frac{1}{4}\right)L, \\ \frac{16}{L^2}\left(\frac{L}{2}-x\right), & \left(k+\frac{1}{4}\right)L \le x \le \left(k+\frac{1}{2}\right)L, \\ 0, & \left(k+\frac{1}{2}\right)L \le x \le (k+1)L. \end{cases} \tag{12}$$

By way of example in Fig. 1 the measured Casimir force is presented together with experimental uncertainties acting between a corrugated plate and a sphere [22]. In the same figure the theoretical results computed by Eqs. (2)–(4) are shown by the curves 1 (uniform distribution), 2 (distribution of Eq. (11)), 3 (distribution of Eq. (12)), and 4 (the bottom of the sphere is over the maximum of corrugation at all times). It is seen that the curve 3 is in agreement with experimental data in the limits of given uncertainties $\Delta F = 5\,\mathrm{pN}$, $\Delta a = 5\,\mathrm{nm}$. The root mean-square average deviation between theory and experiment within the range $169.5\,\mathrm{nm} \leq a \leq 400\,\mathrm{nm}$ (62 experimental points) where the perturbation theory (4) is applicable is $\sigma = 20.28\,\mathrm{pN}$ for the curve 1, $\sigma = 8.92\,\mathrm{pN}$ (curve 2), $\sigma = 4.73\,\mathrm{pN}$ (curve 3), and $\sigma = 9.17\,\mathrm{pN}$ (curve 4). By this means perturbation theory with account of the lateral Casimir force can be made consistent with experimental data.

In conclusion, it may be said that the lateral projection of the Casimir force in a configuration of a sphere above a corrugated plate is examined. It was shown that under the influence of this force the sphere tends to change its position in the direction of a nearest point of stable equilibrium which coincides with a corrugation maximum. This effect makes reasonable the suppositions about different probability distributions describing location of a sphere above a corrugated plate. A particular distribution is suggested which leads to agreement of the perturbation theory and experimental data representing the nontrivial boundary dependence of the Casimir force. The final solution of the problem may be achieved in the experiment where both the vertical and the lateral Casimir force are measured.

ACKNOWLEDGMENTS

The authors are greatly indebted to U. Mohideen for supplying them with original experimental data and V. M. Mostepanenko for several helpful discussions. G.L.K. is grateful to the Centro Brasileiro de Pesquisas Físicas where this work was performed for kind hospitality. She was supported by FAPERJ.

---

[1] H. B. G. Casimir, Proc. Kon. Nederl. Akad. Wet. **51**, 793 (1948).
[2] V. M. Mostepanenko and N. N. Trunov, *The Casimir Effect and Its Applications* (Clarendon, Oxford, 1997).
[3] S. K. Lamoreaux, Phys. Rev. A **59**, R3149 (1999).
[4] A. Lambrecht and S. Reynaud, Eur. Phys. J. D **8**, 309 (2000).
[5] G. L. Klimchitskaya, U. Mohideen, and V. M. Mostepanenko, Phys. Rev. A **61**, 062107 (2000).
[6] V. B. Bezerra, G. L. Klimchitskaya, and V. M. Mostepanenko, Phys. Rev. A **62**, 014102 (2000).
[7] M. Boström and Bo E. Sernelius, Phys. Rev. Lett. **84**, 4757 (2000).
[8] C. Genet, A. Lambrecht, and S. Reynaud, Phys. Rev. A **62**, 012110 (2000).
[9] M. Bordag, B. Geyer, G. L. Klimchitskaya, and V. M. Mostepanenko, Phys. Rev. Lett. **85**, 503 (2000).
[10] G. L. Klimchitskaya, A. Roy, U. Mohideen, and V. M. Mostepanenko, Phys. Rev. A **60**, 3487 (1999).
[11] V. B. Bezerra, G. L. Klimchitskaya, and C. Romero, Phys. Rev. A **61**, 022115 (2000).
[12] G. L. Klimchitskaya and V. M. Mostepanenko, Comm. Mod. Phys. **1**, 285 (2000).
[13] S. K. Lamoreaux, Phys. Rev. Lett. **78**, 5 (1997).
[14] U. Mohideen and A. Roy, Phys. Rev. Lett. **81**, 4549 (1998).
[15] A. Roy, C. Y. Lin, and U. Mohideen, Phys. Rev. D **60**, R111101 (1999).
[16] B. W. Harris, F. Chen, and U. Mohideen, quant-ph/0005088; Phys. Rev. A, 2000, to appear.
[17] M. Bordag, B. Geyer, G. L. Klimchitskaya, and V. M. Mostepanenko, Phys. Rev. D **58**, 075003 (1998).
[18] J. C. Long, H. W. Chan, and J. C. Price, Nucl. Phys. B **539**, 23 (1999).
[19] M. Bordag, B. Geyer, G. L. Klimchitskaya, and V. M. Mostepanenko, Phys. Rev. D **60**, 055004 (1999).
[20] M. Bordag, B. Geyer, G. L. Klimchitskaya, and V. M. Mostepanenko, Phys. Rev. D **62**, R011701 (2000).
[21] V. M. Mostepanenko and M. Novello, hep-ph/0008035.
[22] A. Roy and U. Mohideen, Phys. Rev. Lett. **82**, 4380 (1999).
[23] R. Golestanian and M. Kardar, Phys. Rev. Lett. **78**, 3421 (1997).
[24] R. Golestanian and M. Kardar, Phys. Rev. A **58**, 1713 (1998).
[25] M. Kardar and R. Golestanian, Rev. Mod. Phys. **71**, 1233 (1999).
[26] J. Blocki, J. Randrup, W. J. Swiatecki, and C. F. Tsang, Ann. Phys. (N.Y.) **105**, 427 (1977).
[27] S. I. Zanette, O. Caride, G. L. Klimchitskaya, V. B. Nunes, F. L. Freire Jr., and R. Prioli, Surf. Sci. **453**, 75 (2000).
[28] I. S. Gradshtein and I. M. Ryzhik, *Tables of Integrals, Series and Products* (Academic Press, New York, 1980).

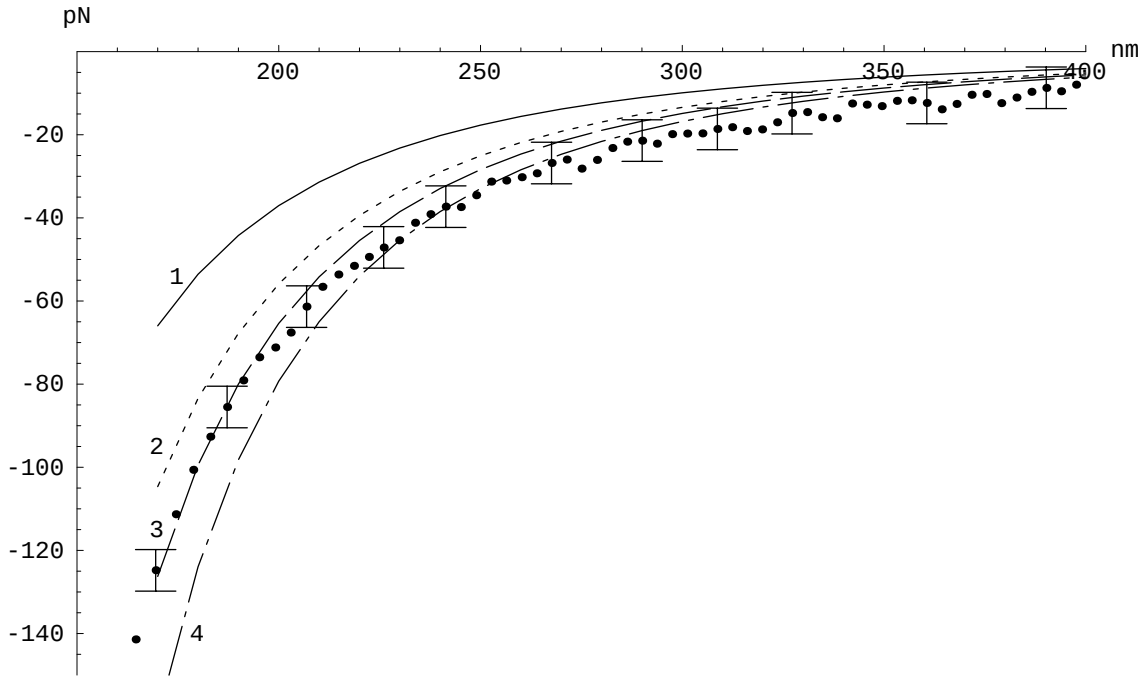

FIG. 1. The Casimir force $F(a)$ from Eq. (2) as a function of the surface separation in configuration of a sphere above a corrugated disk. Curve 1 represents the computational results obtained with the uniform probability distribution, curve 2 — with the distribution of Eq. (11), curve 3 — of Eq. (12), and curve 4 — for a sphere situated above the points of stable equilibrium. Solid circles represent experimental data.